Systemic Modeling of Chaotic EEG During Human Sleep

Mahmoud Alipour
Amirkabir University of Technology
Seyed Mohammad Reza Hashemi Gholpayeghani (m.r.hashemig@aut.ac.ir)
Amirkabir University of Technology

Research Article

Keywords: EEG, Chaos, Nonlinear analysis, Sleep EEG dynamics, Sleep attractor, Sleep cycle

Posted Date: August 25th, 2021

DOI: https://doi.org/10.21203/rs.3.rs-827619/v1

Systemic modeling of chaotic EEG during human sleep

Mahmoud Alipour [a], Seyed Mohammad Reza Hashemi Gholpayeghani [a,*]

[a] Complex Systems and Cybernetic Control Lab, Biomedical Engineering Department, Amirkabir University of Technology, P.O. Box 1591634311, Tehran, Iran. Tel.: (+98) 2164542351.

[*] Corresponding author:

Seyed Mohammad Reza Hashemi Gholpayeghani

Complex Systems and Cybernetic Control Laboratory, Biomedical Engineering Faculty, AmirKabir University of Technology, P.O. Box 1591634311, Tehran, Iran

Tel.: (+98) 2164542351

E-mail: m.r.hashemig@aut.ac.ir

Abstract: One of the most challenging discussions about EEG is the chaotic nature of this biological signal. In the present study, we attempt to provide an analysis to demonstrate sleep EEG chaoticity. We model changes of sleep attractor dynamic in phase space by exponential regression. Our model demonstrates that the sleep attractor is the sleep cycle attractor whose size shrinks during successive cycles by presenting a new definition of the sleep cycle. We study the EEG dynamics of different sleep stages by presenting two new features based on phase space properties. We show that each stage has a unique chaotic attractor. We model geometric changes of these attractors during successive sleep cycles. Our model achieves an accuracy, sensitivity, and specificity of 89.15%, 82.84%, and 81.62% classifying sleep stages.

Keywords: EEG, Chaos, Nonlinear analysis, Sleep EEG dynamics, Sleep attractor, Sleep cycle

1. Introduction

1.1. Background and Motivation

Chaos theory describes the behavior of dynamical systems whose states evolve with time and are highly sensitive to initial conditions [1]. The first thoughts on using chaos theory in EEG analysis can be seen in Basar's work in 1983 [2]. For the first time, Babloyantz attempted to show the EEG's chaotic behavior during the sleep cycle in 1985 [3]. He calculated the complexity of the EEG by its correlation dimension (CD). Other researches in this field performed by Lutzenberger et al. and Natarajan et al. examined the EEG's chaoticity during various brain activities using nonlinear features such as fractal dimension (FD) and CD [4, 5]. Some researchers have also investigated EEG's chaos during sleep [6-8]. Despite these justifications, some researchers believe that the given reasons for EEG's chaoticity are insufficient. For example, they have shown that the positive largest Lyapunov exponent (LLE), non-integer value of the CD, or even the convergence of a time series's CD can be represented by stochastic processes [9-11].

In the time evolution of nonlinear dynamics, the system is often not accessible as a closed formula. However, a trajectory path can show its dynamic in a mathematical space called the phase space [12]. Phase space can display all possible states of the system based on the system's variables or degrees of freedom [13]. Some nonlinear methods, such as the Lyapunov exponents, are based on this space for calculation [14]. A strange attractor is an attractor in phase space that has a fractal structure [15]. A strange attractor is a bounded region of phase space that initially close trajectories separate exponentially such that the

motion becomes chaotic [16]. A strange attractor is one of the key features of a chaotic system [17]. Grassberger and Procaccia studied the CD to measure the strangeness of a chaotic system [14]. Several kinds of research demonstrate EEG chaoticity by measuring EEG attractor's dimensional complexity by nonlinear tools such as CD and FD [7, 18, 19]. In addition to examining EEG's nonlinear properties by plotting this signal in the phase space at different sleep stages, some studies tried to show its chaotic nature [3, 18].

For our study, we select 20 subjects from the Sleep-EDF Database Expanded [20], a greatly expanded version of Sleep-EDF Database [21], which is a popular dataset in sleep stages modeling [22-25]. Similar to previous researches [3-5], some studies used nonlinear features to show the chaos of EEG in the Sleep-EDF Database [18, 26]. Also, some studies used nonlinear features for sleep stage classification in this dataset [27-29].

1.2. Contribution and Paper Organization

This paper tries to study the attractors of sleep EEG and its stages in phase space during successive cycles. We want to state that the sleep EEG is a chaotic signal with a strange attractor, and each sleep stage has a strange attractor inside a general sleep attractor. Based on our knowledge, no study presents a unique solution or feature to derive chaos in EEG, which a stochastic signal cannot represent. Therefore, our goal is to demonstrate that contrary to stochastic signals, the attractors of sleep EEG and its stages have a geometrical structure changing according to a specific pattern during successive cycles. Continuing the previous attempts to show chaos in EEG [18, 26], we believe this pattern can illustrate EEG chaoticity and separate it from stochastic signals. Because the brain is a complex system [30], we study the sleep phenomenon from a system theory perspective which tries to explain complex system dynamics [31].

Behavioral complexity measurement is a way of studying complex system dynamics [32]. Because of EEG's nonlinear nature [19], we use nonlinear analysis to examining EEG complexity. We present two nonlinear features that can measure the system's complexity based on the geometric arrangement of EEG attractor points in phase space.

Section 2 explains our specific procedure about determining sleep cycles which has an essential role in determining the relationship between stages and their attractors. Section 3 introduces our new features and employed statistical tests. Section 4 presents the experimental results. This section shows that the sleep cycle's attractor shrinks during successive cycles by beginning the sleep process. We model variations of sleep attractor size by exponential regression. Then we model the stages attractors dynamics by providing simple time-dependent mathematical relationships. For evaluation, we implement a sleep stages classification and report its performance. Section 5 discusses our approaches to show EEG chaoticity and modeling stages attractors. Finally, section 6 gives a conclusion of our study.

2. Materials

The data used in this study is polysomnographic recordings of 20 healthy subjects (10 male and 10 female, aged 25 to 34 years old). Data recorded for two successive nights (a recording of a single subject is not available) selected from Sleep-EDF Database Expanded has been used [20]. Each recording contains information about more than 20 hours of biological signals. EEG recordings of data consist of two channels, Fpz-Cz and Pz-Oz. Since we aim to study the sleep dynamics based on a single EEG channel, we use the Fpz-Cz

channel. We use this channel due to the Fpz-Cz channel's superiority over the Pz-Oz channel to detect sleep stages [33, 34]. We used the 12th order Butterworth notch filter at 50 Hz to remove power line interference. Experts prepared the hypnogram of data according to the R&K manual in 30-second epochs. To use the AASM manual, we considered the third and fourth stages of the R&K manual as the third stage of the AASM manual. There were 58 movement epochs in only 17 of the 39 recordings. We remove these epochs because experts did not score them as any of the five sleep stages based on AASM manual recommendation [35].

2.1. Data preparation

Due to the lack of specific patterns in the occurrence of sleep stages or their repetition, different sleep cycle definitions have been proposed [36]. Also, we found that the limitation of the definition of the sleep cycle in literature causes a portion of data lost in our analysis. In some research, the 5-minute succession of REM stages is a requirement for defining a sleep cycle [36, 37]. However, in some cases in our dataset, there is no succession of REM stages in sleep cycles for a constant time. Hence, without changing the main concept of sleep and its cycle definition, we define a term called complete sleep, which includes one or more complete sleep cycles. A complete cycle means the continuous occurrence of non-rapid eye movement stages (NREM period) for at least 5 minutes and the rapid eye movement stages (REM period) for at least 5 minutes, respectively. This definition is similar to the complete sleep cycle definition of reference [36]; the difference is that in the present study, we consider the minimum duration of the NREM period to be at least 5 minutes instead of at least 15 minutes. Also, we present another condition for defining a complete

cycle to make this definition more comprehensive. We accept REM stages mixed with other stages for at least 5 minutes as the end of a cycle, if the first, the end, and most of the epochs of this duration be REM stage. If the subject wakes up during the REM period, we accept the last sleep cycle with any REM period length as a complete sleep cycle.

An essential issue in the present study is that we may consider more than one complete sleep for a subject in one night's sleep. This condition may happen when a subject waked up for a while during a night's sleep. In our work, we define the end of sleep with three conditions: First, the occurrence of waking epochs along with other sleep stages for more than 10 minutes, while the first, the end, and most epochs of this duration be waking stages. Second, waking up for more than an hour during sleep, and third, waking up for more than half an hour during the REM period. In the third case, when waking epochs occurs during the REM period, we consider the two REM periods together as the last cycle's REM period by eliminating the waking time. In the present data, three subjects have more than one complete sleep.

2. 2. Elimination of waking epochs during sleep

To eliminate waking epochs, we follow the method provided by reference [37]. The stage that occupies more than half of the epoch length determines the label of that epoch [35]. Also, waking up and falling asleep could not have happened instantaneously. Therefore, in this study, waking epochs and their pre-epochs and post-epochs were removed from the EEG data to eliminate the effects of waking on other stages as far as possible.

3. Methods

EEG epochs are signals with fixed lengths of 3000 samples that a sleep expert labels. To study these epochs, we present features that can extract their complexity information. To evaluate features' performance to discriminate between stages epochs, we introduce appropriate statistical tests. Section 3.3 describes our approach for studying subjects' sleep EEG with different duration to reveal sleep EEG patterns.

3. 1. Feature extraction

The proposed features in this study need phase space for calculation. Phase space reconstruction requires calculating the system dimension equivalent to the phase space dimension and system time delay. One of the most common methods for calculating system dimensions is the false nearest neighbor method [38]. The average mutual information method is a conventional method for calculating the optimal delay [39]. The coordinates of each point (X_i) in this space are according to Eq. (1).

$$X_i = (x_i, x_{i+\tau}, \ldots, x_{i+(m-1)\tau}) \quad (1)$$

In Eq. (1), x is the EEG signal, m is the optimal dimension, and τ is the optimal time delay. We design our proposed methods in the two-dimensional (2D) phase space to reduce the computational load.

3. 1. 1. Phase change method

This method calculates the phase changes (PC) between the phase space points after reconstructing the EEG in phase space. The phase between two points (θ_i) in the phase

space is the angle between the lines that connect two successive points to the origin point (0,0), according to Fig. 1 and Eq. (2). In this relation, D_i is the distance between a point in the phase space and the origin point, and C_i is the distance between two successive points of the phase space.

$$PC = \sum_{i=1}^{n-1} \theta_i = \sum_{i=1}^{n-1} \left|\cos^{-1} \frac{{D_i}^2 + {D_{i+1}}^2 - {C_i}^2}{2 D_i D_{i+1}}\right| \quad (2)$$

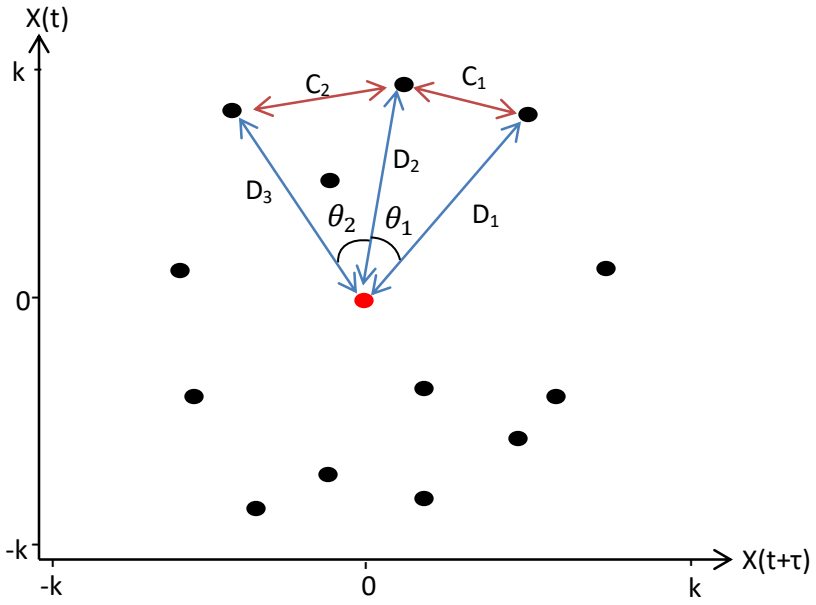

Figure 1. Reconstruction of a hypothetical EEG signal in phase space. Equation (2) is the sum of the angles between successive points and the origin point ($\sum_{i=1}^{n} \theta_i$). The red point is the origin of phase space.

3. 1.2. Changes in distance from the origin of phase space

In this method, after signal reconstruction in phase space, each point's Euclidean distance to the origin point (D_i) is calculated, according to Fig. 1. Then these distances are added

together, according to Eq. (3). In Eq. (3), $(x(i), x(i+\tau))$ is the coordinates of the signal reconstructed points in phase space, n is the signal's length, and τ is the time delay. From now on, we call this feature changes in distance from the origin (CDO).

$$CDO = \sum_{i=1}^{n-\tau} D_i = \sum_{i=1}^{n-\tau} \sqrt{x(i)^2 + x(i+\tau)^2} \quad (3)$$

The first and second row of Fig. 2a intuitively demonstrates the CDO and PC methods' ability by applying them to the EEG for 300 minutes before and after nighttime sleep. Figure. 2b shows the result by removing waking epochs. As Fig. 2b shows, we see a specific pattern in the first subject's EEG behavior. The first row of Fig .2b shows that in each sleep cycle, CDO increases with the beginning of the cycle according to sleep depth and decreases when it approaches the end of the NREM period. CDO has its lowest values in the cycle during the REM period. The second row of Fig. 2b shows an inverse trend for the PC method.

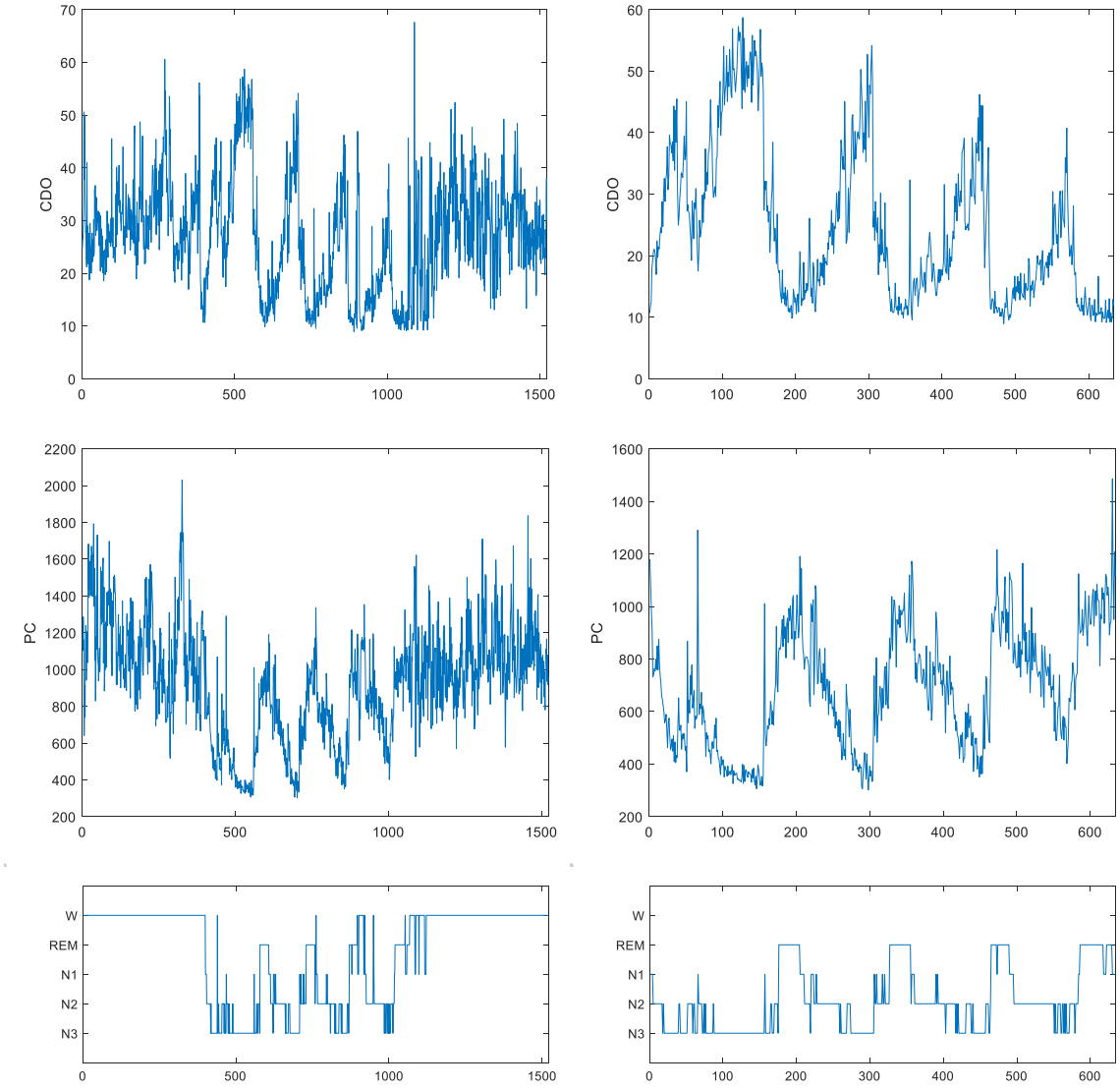

Figure 2. Result of applying the CDO and PC methods accordingly in the first and second rows. (a) Appling the proposed methods to the EEG of the first night of the first subject with considering wake epochs from 300 minutes before falling asleep and after waking up, (b) the result of applying the methods on the EEG with eliminating wake epochs. The subject's

sleep duration is 721 epochs (considering wake epochs), equivalent to 6 hours. The third row shows the hypnogram of data.

3.2. EEG analysis in sleep cycles

To investigate sleep EEG, we analyze CDO and PC values' changes in each subject's cycles. Due to the variability of cycle length, we scale the length of cycles in the same way. To scale the length of REM and NREM periods in each cycle, we consider the REM and NREM period's duration fixed at 20 minutes (40 30-second epochs) and 70 minutes (140 30-second epochs), respectively. For the NREM period, we perform a 140-point interpolation between each two successive CDO values. Then we perform a down sampling at a rate equal to the NREM period's time duration in each cycle to obtain a 140-point (70-minute) signal. Due to the variability in the CDO's amplitude range for each subject, we scale it in the range of $[0, 1]$. We perform the same process for the REM period to obtain a 40-point signal. With the end of the nighttime sleep, frequent intermittent between waking and REM stage occurs [40]. Discontinuity in the REM period causes difficulty accurately determining the sleep cycles (four subjects in the present study have more than five sleep cycles). Therefore we limit our study to subjects' first five sleep cycles.

3.3. Statistical tests

We use two statistical tests in this study: Mann–Whitney U-test and Kolmogorov–Smirnov (KS) test. Wilcoxon–Mann–Whitney U-test test or U-test is a nonparametric test of the null hypothesis that selected data x and y from two populations, samples from continuous distributions with equal medians, against the alternative that they are not. The U test assumes that x and y are independent [41]. U-test is more robust than the t-test to indicate

significance inaccurately because of the presence of outliers [42]. For distributions far from normal and large sample sizes, the U-test is considerably more efficient than the t-test [43]. KS test is a nonparametric test that tests whether the data in vector x comes from a normal distribution or not [44]. This test decides to reject the null hypothesis by comparing the p-value with the significance level α. In this study, we consider the significance level α equal to 5%.

4. Results

This section shows the result of extracting proposed features from EEG and considering the labels of epochs as REM and NREM. With this approach, we show the general pattern of the EEG NREM period during successive cycles. We model maximum NREM variation in successive cycles with an exponential regression. We demonstrate the performance of our model by reporting regression errors. After that, we reveal the sleep stages' EEG patterns and model their dynamics. By performing leave one out cross-validation, we report the sleep stages classification model's accuracy, sensitivity, and specificity.

4.1 Sleep EEG dynamic

Figure 3 shows the CDO's and PC's mean and standard deviation of NREM and REM periods for all subjects in the first five successive cycles after applying the method of EEG analysis in section 3.3. As shown in the successive cycle, Fig. 3a shows the decreasing trend of the maximum amplitude of the CDO, and Fig. 3b shows the increasing trend of the

minimum amplitude of the PC. As Fig. 3 shows, we see a similar pattern in all cycles. These patterns are the average behavior of all subjects.

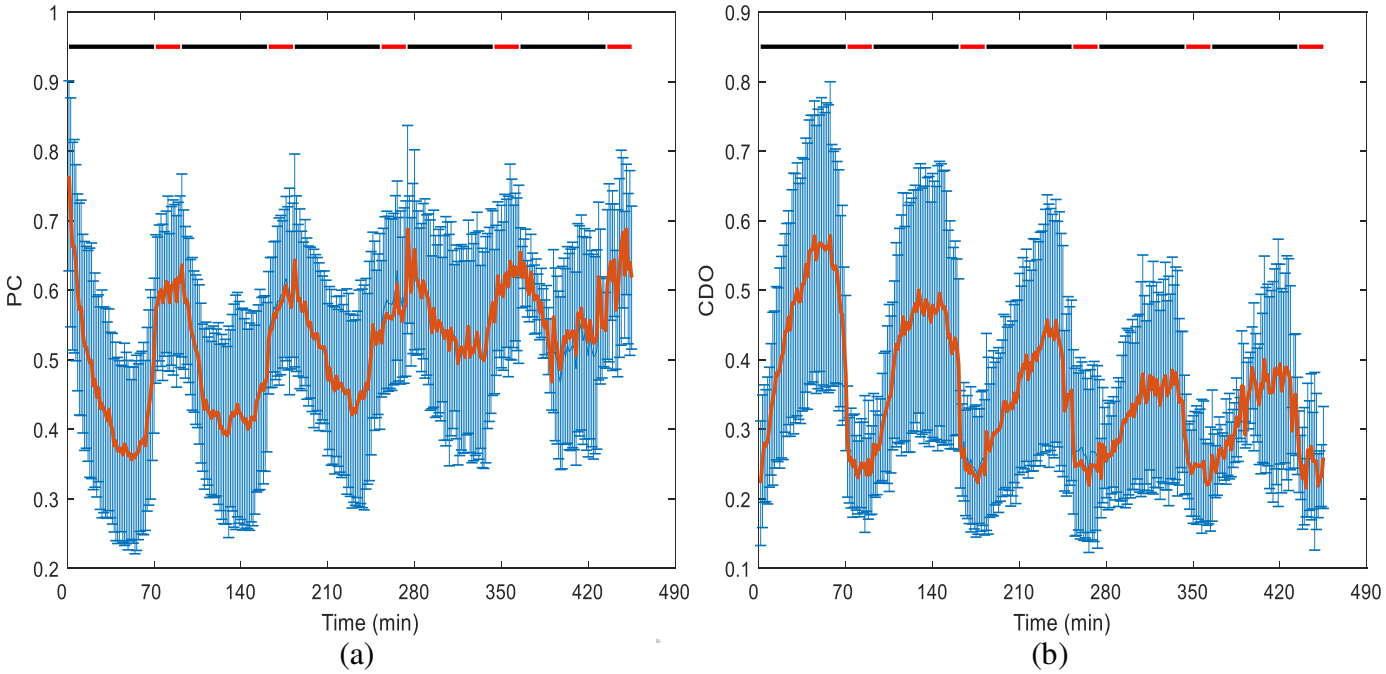

Figure 3. (a) and (b) are mean (brown) and standard deviation (blue) of PC and CDO, respectively, in 5 successive cycles. The black and red line above the figure shows the NREM and REM period, respectively. The length of all cycles is 90 minutes (70 minutes for NREM and 20 minutes for REM).

Table 1 shows the mean and standard deviation of stages' CDO and PC values in successive cycles. In each cycle, the CDO's mean increase, and PC's mean decrease by increasing the depth of sleep. Thus, the CDO's highest and lowest values in each cycle are related to stage 3 and REM, respectively. Conversely, each cycle's lowest and highest PC values are related to stage 3 and REM, respectively. Table 1 shows that the distance between the phase space's

trajectory and origin increases with sleep depth. Near the end of the cycle and simultaneously with decreasing sleep depth, this distance decreases. PC shows a reverse pattern. This repetitive behavior of EEG trajectories shows that the sleep attractor shrinks during successive cycles. In other words, the area in which the trajectory moves in phase space shrinks.

Table 1. Mean and standard deviation of CDO and PC for different stages during successive cycles of all subjects. Before averaging, the values of each feature scaled in the range of $[0, 1]$.

Stage	Feature	Cycle 1	Cycle 2	Cycle 3	Cycle 4	Cycle 5
1	CDO	0.2528±0.0565	0.2845±0.0820	0.2672±0.0771	0.2701±0.0890	0.2791±0.0744
	PC	0.5535±0.0792	0.5304±0.0664	0.5478±0.0604	0.5577±0.0661	0.5862±0.1022
2	CDO	0.3825±0.0613	0.3497±0.0625	0.3384±0.0992	0.3173±0.0656	0.3169±0.0478
	PC	0.6111±0.0462	0.5948±0.0474	0.5852±0.0561	0.5857±0.0472	0.5978±0.0429
3	CDO	0.6302±0.1209	0.5707±0.1216	0.5707±0.1216	0.5401±0.1083	0.5736±0.1373
	PC	0.5989±0.0590	0.5683±0.0529	0.5683±0.0529	0.5727±0.0576	0.5613±0.0575
REM	CDO	0.2465±0.0488	0.2540±0.0729	0.2656±0.1112	0.2385±0.0438	0.2534±0.0472
	PC	0.6200±0.0714	0.6107±0.0699	0.5979±0.0820	0.5981±0.0550	0.6020±0.0569

4.1.1. Sleep attractor modeling

Figure 4 shows the fitted line on the mean of more than 95% of the CDO's maximum amplitude ($meanCDOmax_{95\%}$) and less than 5% of the PC's minimum amplitude ($meanPCmin_{5\%}$) in the NREM period of the successive cycles. The horizontal axis and vertical axis are in terms of cycle number and logarithmic values in this figure. According to Fig. 4, we can consider that the $meanCDOmax_{95\%}$ in successive cycles decreases with the slope $e^{\frac{-C}{\tau_a}}$. The parameter C is the cycle number. The parameter τ_a is the CDO decreasing

constant, which is equal to 9.524. As a result, $A_0 e^{\frac{-C}{\tau_a}}$ shows the average maximum CDO after the first cycle can. Parameter A_0 is the $meanCDOmax_{95\%}$ in the first cycle. For the PC feature, $B_0 e^{\frac{C}{\tau_b}}$ shows the average minimum PC after the first cycle. Parameter B_0 is the $meanPCmin_{5\%}$ in the first cycle. The parameter τ_b is the PC increasing constant, which is equal to 10.021.

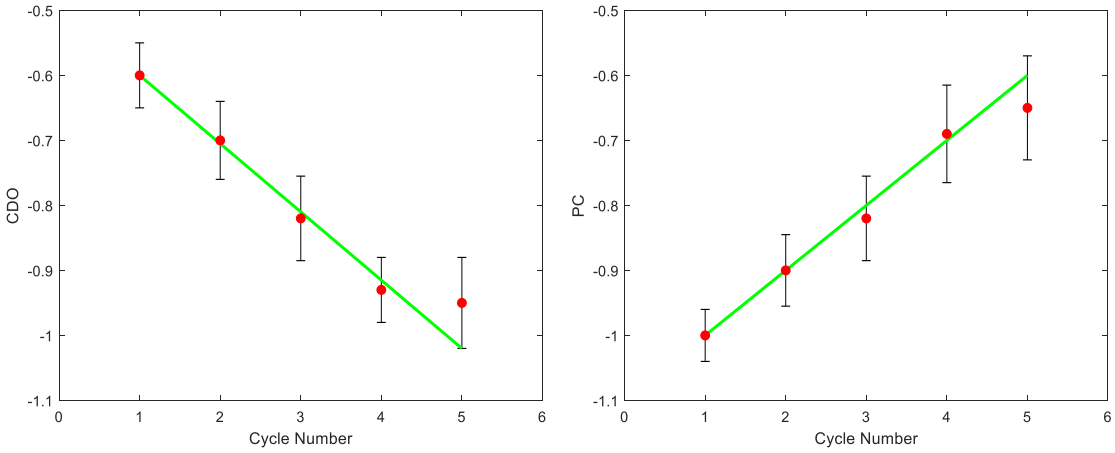

(a) (b)

Figure 4. (a) and (b) are mean (red) and standard deviation (black) of $meanCDOmax_{95\%}$ and $meanPCmin_{5\%}$ of NREM period during successive cycles of all subjects. The vertical axis is logarithmic. The horizontal axis shows the cycle number. The green line represents the fitted line.

4.1.2. Sleep model evaluation

First, we normalize subjects' CDO and PC values between $[0, 1]$. Then we fit our exponential regression model on $meanCDOmax_{95\%}$ in successive cycles for all subjects. With a 95% prediction interval, the standard error for the regression is $6.83\% \pm 1.33\%$. The

mean and standard deviation of mean square error (MSE) for all subjects is 0.061 ± 0.014. With the same prediction interval, the standard error for the regression on $meanPCmin_{5\%}$ is $7.16\% \pm 2.15\%$. The mean and standard deviation of MSE of this model is 0.082 ± 0.024.

4.2. Sleep stages dynamics

Now we want to survey this question: whether the trajectory in each stage moves in a determined place in the sleep attractor or moves throughout this attractor randomly?

KS test shows that from the first to fifth cycle, with a significance level of 5% in 94.64%, 82.74%, 79.17%, 79.35%, and 75% of cases, the distribution of CDO's amplitude values are not normal. On average, the CDO's distribution of stages within the cycles is not normal. In non-normal data, the median is more appropriate than the mean for averaging [45]. So, we use the median for investigating average changes in CDO's values.

To detect attractors of sleep stages, we have to determine the bounds of stages. Bounds of stages are the CDO's minimum and maximum amplitude values. Therefore, in addition to the CDO's median, we examine CDO's minimum and maximum values to show their distinguishability in different stages. In advance, to investigate the distinguishability of CDO's minimum, median and maximum (CDOMMM), it is essential to check the normality of their distribution.

To Determine the central tendency of CDOMMM for each stage, we use the KS test result to specify the type of averaging method. Table 2 shows the p-values of the KS test with a significance level of 5% for CDOMMM. This table shows that the distributions of

CDOMMM are not normal in stages of successive cycles for all subjects. Therefore, we will use the medians of CDOMMM to determine their central tendency for stages.

Table 2. The p-values of the KS test with a significance level of 5% for CDOMMM of stages in different cycles.

Cycle	Stage	Min	Median	Max
1	1	1.65E-14	2.19E-11	4.75E-17
	2	3.57E-15	5.11E-14	5.16E-21
	3	1.22E-15	1.37E-15	6.93E-18
	REM	1.92E-15	5.08E-12	5.10E-19
2	1	7.23E-12	1.58E-09	5.63E-13
	2	3.15E-15	9.12E-14	5.37E-21
	3	7.32E-14	5.79E-14	8.31E-16
	REM	3.86E-15	4.50E-12	1.33E-18
3	1	2.93E-10	2.70E-08	8.06E-12
	2	2.52E-13	3.02E-11	4.06E-16
	3	1.40E-11	6.04E-11	1.43E-12
	REM	1.22E-11	7.46E-11	2.36E-15
4	1	4.33E-08	4.63E-06	3.11E-09
	2	1.53E-08	2.77E-07	5.92E-12
	3	7.74E-07	2.86E-06	1.58E-07
	REM	8.61E-09	2.42E-07	7.80E-12
5	1	0.00088	5.04E-03	0.00023
	2	0.00038	1.14E-03	3.10E-06
	3	0.00135	1.80E-03	0.00092
	REM	0.00064	2.58E-03	2.13E-05

According to the non-normal distribution of values in Table 2, the U-test is suitable to evaluate the distinguishability of stages' CDOMMM. Table 3 shows the p-values of the U-test between stages in different cycles for the CDOMMM. For obtaining the stages' CDOMMM, due to their non-normal distribution, the outlier data is removed with the Tukey outlier data removal method [46]. Values of p-value> 0.05 are in boldface in Table 3. As this table shows, the CDO feature could not distinguish between stage one and REM. Also,

the minimum CDO values of stages show high similarity between stage one and stage 2. Based on the high correlation of stages one and REM CDO values, we ignore stage one from our modeling and focus on stages 2, 3, and REM.

Table 3. U-test p-values with a significance level of 5% between stages' CDOMMM in successive cycles. P-values greater than 0.05 are in boldface.

Cycle	Stage	Min				Median				Max			
		S1	S2	S3	SR	S1	S2	S3	SR	S1	S2	S3	SR
1	S1	1	4.8E-07	1.2E-14	**0.6521**	1	8.1E-11	9.3E-14	**0.6652**	1	2.1E-12	1.1E-14	**0.9673**
	S2	4.8E-07	1	1.3E-14	1.7E-08	8.1E-11	1	4.2E-08	3.7E-12	2.1E-12	1	5.4E-13	1.4E-13
	S3	1.2E-14	1.3E-14	1	6.8E-15	9.3E-14	4.2E-08	1	2.5E-14	1.1E-14	5.4E-13	1	6.8E-15
	SR	**0.6521**	1.7E-08	6.8E-15	1	**0.6653**	3.7E-12	2.5E-14	1	**0.9673**	1.4E-13	6.8E-15	1
2	S1	1	**0.5116**	6.6E-12	0.0166	1	0.0001	2.9E-11	**0.2786**	1	0.0008	2.6E-12	**0.0907**
	S2	**0.5116**	1	4.2E-14	3.8E-06	0.0001	1	3.0E-09	1.8E-09	0.0008	1	6.4E-13	5.8E-10
	S3	6.6E-12	4.2E-14	1	1.1E-13	2.9E-11	3.0E-09	1	5.0E-13	2.6E-12	6.4E-13	1	1.4E-13
	SR	0.0166	3.8E-06	1.1E-13	1	**0.2786**	1.8E-09	5.0E-13	1	**0.0907**	5.8E-10	1.4E-13	1
3	S1	1	**0.4690**	2.4E-10	**0.1212**	1	1.4E-06	5.9E-09	**0.3332**	1	0.0031	3.3E-10	**0.8127**
	S2	**0.4690**	1	8.0E-11	0.0026	1.4E-06	1	8.4E-06	1.7E-06	0.0031	1	1.1E-09	4.4E-06
	S3	2.4E-10	8.0E-11	1	8.0E-11	5.9E-09	8.4E-06	1	1.2E-09	3.3E-10	1.1E-09	1	9.6E-11
	SR	**0.1212**	0.0026	8.0E-11	1	**0.3332**	1.7E-06	1.2E-09	1	**0.8127**	4.4E-06	9.6E-11	1
4	S1	1	**0.2415**	2.0E-06	0.0472	1	0.0062	0.0002	**0.7058**	1	0.0078	1.7E-06	**0.2011**
	S2	**0.2415**	1	3.6E-07	0.0014	0.0062	1	0.0016	0.0005	0.0078	1	7.8E-06	5.0E-05
	S3	2.0E-06	3.6E-07	1	2.8E-07	0.0002	0.0016	1	6.5E-06	1.7E-06	7.8E-06	1	2.8E-07
	SR	0.0472	0.0014	2.8E-07	1	**0.7058**	0.0005	6.5E-06	1	**0.2011**	5.0E-05	2.8E-07	1
5	S1	1	**0.5414**	0.0003	0.0273	1	**0.1995**	0.0093	**1**	1	**0.1995**	0.0003	**0.5414**
	S2	**0.5414**	1	0.0001	0.0625	**0.1995**	1	0.0417	0.0314	**0.1995**	1	0.0001	0.0053
	S3	0.0003	0.0001	1	0.0001	0.0093	0.0417	1	0.0020	0.0003	0.0001	1	0.0001
	SR	0.0273	0.0625	0.0001	1	**1**	0.0314	0.0020	1	**0.5414**	0.0053	0.0001	1

Figure 5 shows the fitted line on the medians of CDOMMM's box plots for stages 2, 3, and REM in successive cycles. This figure shows CDOMMM's changes during sleep have a pattern. The minimum and maximum CDO values determine the stage attractor's bounds distinct from other attractors. The general sleep attractor consists of a combination of stages

attractors. The CDO median values pattern of each stage shows the average trajectory behavior in the general sleep attractor. Figure 5 shows medians of CDOMMM of stage 2, which decrease during successive cycles. For stage 3, the CDO's median and maximum variation trend descends while CDO's minimum has ascending trend during successive cycles. The median and minimum of CDO of the REM stage have a downward trend during successive cycles, while the CDO's maximum has an upward trend. Table 4 shows the fitted lines' slope on the medians of CDOMMM for stages 2, 3, and REM during successive cycles. The interquartile ranges in Table 4 indicate slopes of the median's upper and lower quartiles of CDOMMM.

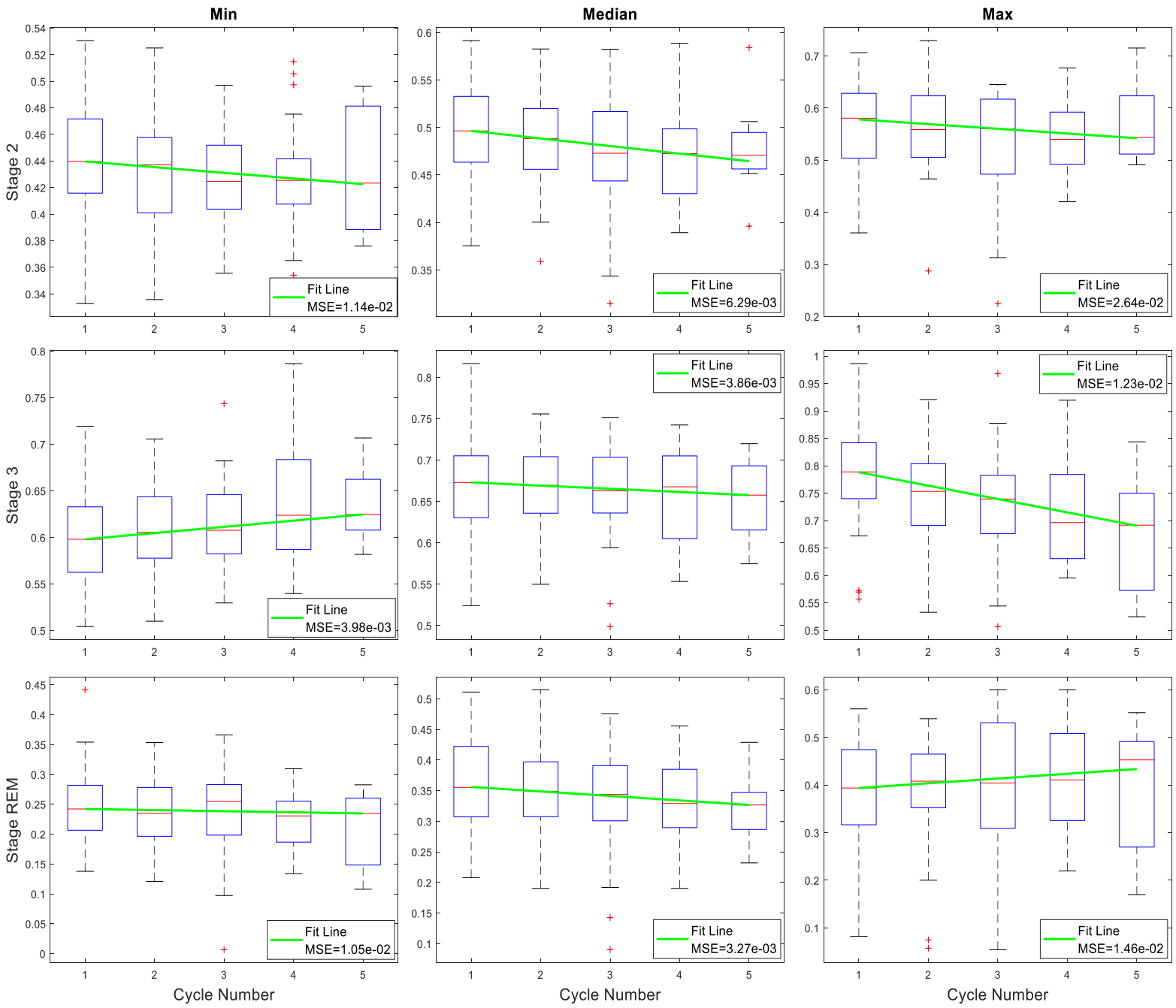

Figure 5. Box plot of changes in the CDOMMM of stages for all subjects during successive cycles. The first to third rows show the changes in stages 2, 3, and REM. The left to right columns corresponds to the minimum, median and maximum changes of CDO. The vertical axis shows the scaled CDO's values, and the horizontal axis shows the sleep cycle number.

The green lines represent the fitted line on the median points. The MSE shows the calculation error inside each subfigure.

Table 4. The slope of fitted lines on the medians of CDOMMM and their interquartile range (in parentheses) for stages 2, 3, and REM for all subjects during successive cycles.

Stage	Minimum	Median	Maximum
2	$-0.0043\ (-0.0038, -0.0049)$	$-0.008\ (-0.006, -0.0012)$	$-0.0090\ (-0.0080, -0.0011)$
3	$0.0067\ (0.0059, 0.0077)$	$-0.0038\ (-0.0032, 0.0042)$	$-0.0244\ (-0.02010, -0.0267)$
REM	$-0.0019\ (-0.0013, -0.0026)$	$-0.0074\ (-0.0065, -0.0080)$	$0.0100\ (0.0098, 0.0108)$

4.2.1. Sleep stages attractors modeling

Figure 6 shows a schematic of the maximum and minimum CDO changes of stages 2, 3, and REM in three consecutive cycles. In this figure, the attractors of stages 2, 3, and REM are considered a disk. L2, L3, and LR are the differences between the maximum and minimum distance of points from the origin of phase space in stages 2, 3, and REM, respectively. They are a symbol of the size of each corresponding sleep stage attractor. According to Table 4, since the maximum slope of the CDO for stage 2 is greater than the minimum slope of the CDO, L2 decreases during successive cycles. Decreasing the maximum and increasing the minimum amplitude of the CDO for stage 3 indicates L3 decreases during successive cycles. The negative and positive slopes of the REM stage's minimum and maximum CDO mean increasing LR. Therefore, the attractor of stages 2 and 3 decreases, while the REM stage's attractor increases during the successive cycles.

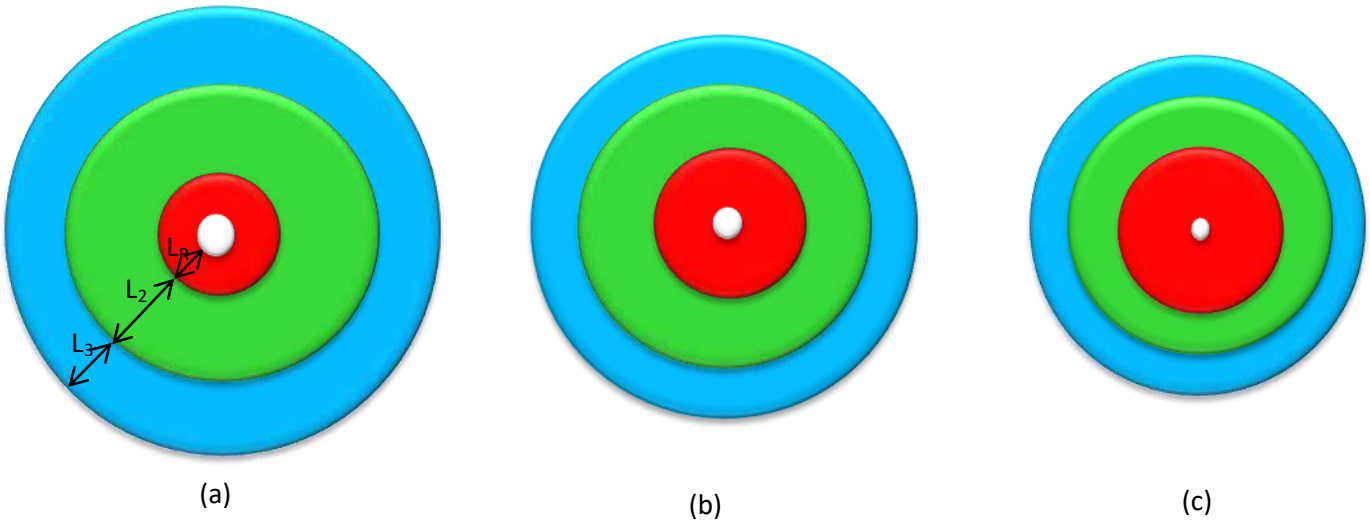

Figure 6. Schematic representation of the changes in CDO's maximum and minimum values for stages 2, 3, and REM in three consecutive cycles. a, b, and c show the area covered by the attractor of stages on the phase space in the first, second, and third cycles, respectively. The attractors of stages 2, 3, and REM are considered a disk with green, blue, and red colors, in which L2, L3, and LR show the difference between the CDO's maximum and minimum values, respectively. The white area inside the red area indicates where the CDO has no value for different stages.

Table 5 shows the mathematical relationships of L2, L3, and LR in Fig. 6. These relationships are dependent on the number of cycles. They are relative to the area in the general sleep attractor in which the trajectory moves at each stage.

Table 5. Mathematical relationships of changes in L2, L3, and LR. The values of $r_{2_{max_0}}$, $r_{3_{max_0}}$, $r_{R_{max_0}}$, and the values of $r_{2_{min_0}}, r_{3_{min_0}}$, and $r_{R_{min_0}}$ show the maximum and minimum CDO values in the first sleep cycle for stages 2, 3, and REM, respectively. Constant parameters of relationships are $(P_{2_{max}}, P_{3_{max}}, P_{R_{max}})$ and $(P_{2_{\min}}, P_{3_{\min}}, P_{R_{\min}})$,

which are maximum and minimum values of CDO slopes of stages 2, 3, and REM in Table 4, respectively. C is the number of sleep cycles.

Size of each stage attractor	The relationship of changing in size of each attractor
L_2	$r_{2_{max_0}}(1+P_{2_{max}}C)-r_{2_{min_0}}(1+P_{2_{min}}C)$
L_3	$r_{3_{max_0}}(1+P_{3_{max}}C)-r_{3_{min_0}}(1+P_{3_{min}}C)$
L_{REM}	$r_{R_{max_0}}(1+P_{R_{max}}C)-r_{R_{min_0}}(1+P_{R_{min}}C)$

4.2.2. Sleep stages model evaluation

For evaluation of the performance of our model, we used it as a sleep stages classifier. We used leave-one-out cross-validation. In the training phase, appropriate $P_{i_{max}}$ and $P_{i_{min}}$ (i=2,3 and REM) have been obtained. Then by use of maximum and minimum CDO in the first cycle of a test subject ($r_{2_{max_0}}$ and $r_{2_{min_0}}$) and using obtained $P_{i_{max}}$ and $P_{i_{min}}$, the model's performance has been evaluated. Our model achieved an average classification accuracy, sensitivity, and specificity of 89.15%, 82.84%, 81.62%, respectively. Table 6 shows the confusion matrix of our classification.

Table 6. Confusion matrix for three-stage sleep classification.

	Stage 2 (Model)	Stage 3 (Model)	Stage REM (Model)	Sensitivity
Stage 2 (Expert)	15208	983	1593	85.52 %
Stage 3 (Expert)	757	4164	128	82.47 %
Stage REM (Expert)	1381	168	6412	80.54%

5. Discussion

Many studies tried to demonstrate EEG chaoticity using nonlinear features [5-8]. In this paper, we attempted to show EEG chaoticity in our dataset using nonlinear features. Chaotic and stochastic signals have similarities in many aspects [9, 10]. Therefore, it is controversial to show EEG chaoticity using conventional approaches to measure EEG nonlinearity [11]. We tried to demonstrate EEG chaoticity from a different view. We revealed a pattern of changes in each stage attractor during successive sleep cycles and demonstrated that sleep EEG is not a stochastic signal but a chaotic signal. This study introduced two nonlinear features based on phase space properties to investigate sleep EEG dynamic in section 4.1 and present trajectory motion specific patterns during sleep stages in section 4.2. Therefore, the sleep strange attractor can be considered the attractor of the repeatable sleep cycle during sleep. However, the size of the strange attractor decreases over successive cycles. Similar to reference [8], Table 1 showed that the proposed features change according to the complexity

of stages. This accordance demonstrates that our features can measure the complexity of EEG epochs. The complexity of EEG reflects interactions of brain neural networks [47], which is related to brain consciousness level [48, 49]. Based on this relationship, we can conclude that our features can measure brain consciousness levels.

Studies modeled sleep in various aspects such as sleep stages classification [24], slow-wave activity [37], and circadian rhythm [50]. This study modeled sleep from a system theory perspective and use EEG reconstruction's geometric properties in phase space. We use just a single EEG channel and a single feature. Our model achieves a sensitivity of 85.52%, 82.47%, and 80.54% in classification stages 2, 3, and REM. In classification stages 2, 3 and REM ,respectively, reference [28] achieves sensitivity of 87.07%, 98.77%, and 83.33% and reference [51] archives sensitivity of 89.56%, 79.85%, and 78.14%. These results reveal that our model has an acceptable performance.

In section 4.1.1, the CDO method demonstrates a similar EEG delta band power pattern, which Achermann et al. modeled [37]. EEG is a non-stationary signal [18], and using of frequency and power of a signal is valid only when a signal is stationary [52]. However, the CDO and PC methods are not dependent on the stationarity of a signal.

One of the limitations that we encountered in our research was the determination of sleep cycles. Defining a sleep cycle is a challenging issue [36]. As the end of nighttime sleep approaches, an increase in light sleep incidence during the REM period makes it difficult to determine sleep cycles accurately [37]. Section 2.1 presents new definitions for the sleep cycle to reduce the limitations of defining it and consider more modes of combining REM

and NREM periods with different lengths. Another issue we encountered in this study was determining complete sleep. We found that prolonged waking during nighttime sleep causes a change in the sleep EEG dynamics. As a result, the descending trend of CDO or ascending trend of PC in successive cycles disturb. However, the mentioned pattern can be seen again by considering sleeping again after prolonged waking as a new complete sleep. In three of the 39 subjects' night data, we identified more than one complete sleep during their nighttime sleep. Therefore, we included two complete periods of sleep for them in nighttime sleep.

EEG activity of stages one and REM are so similar that they are intuitively indistinguishable [53]. Other studies have reported low sensitivity of stage one detection in their work [54, 55]. On the other hand, stage one epochs' volume in a normal night's sleep is 2% to 5% [56, 57]. Section 4.2.1 ignores stage one from our examination and focuses on stages 2, 3, and REM based on these facts. Maybe analyzing EEG epochs in a higher dimension can solve the indistinguishability between stage one and REM's CDO values.

Sleep-EDF Database Expanded has a wide age range (25 to 101 years) and a sufficient number of male and female subjects (78 subjects). Therefore, future studies can analyze the effect of age and sex in the proposed modeling.

6. Conclusion

This study introduced two nonlinear features based on phase space properties to investigate sleep EEG dynamics. We demonstrated and modeled the pattern of trajectory motion during sleep and its stages. The existence of this pattern illustrates that the attractor of sleep EEG

has no resemblance to the attractor of a stochastic signal. Our proposed features can measure the degree of complexity, which helps to reveal chaotic system dynamics. Our sleep stages model based on one of our introduced features can classify sleep stages with acceptable accuracy.

7. References

1. Wang, Z., Z. Liu, and C. Zheng, *Qualitative analysis and control of complex neural networks with delays*. 2016: Springer.
2. Basar, E., *Toward a physical approach to integrative physiology. I. Brain dynamics and physical causality.* American Journal of Physiology-Regulatory, Integrative and Comparative Physiology, 1983. **245**(4): p. R510-R533.
3. Babloyantz, A., J. Salazar, and C. Nicolis, *Evidence of chaotic dynamics of brain activity during the sleep cycle.* Physics letters A, 1985. **111**(3): p. 152-156.
4. Natarajan, K., et al., *Nonlinear analysis of EEG signals at different mental states.* Biomedical engineering online, 2004. **3**(1): p. 1-11.
5. Lutzenberger, W., et al., *The scalp distribution of the fractal dimension of the EEG and its variation with mental tasks.* Brain topography, 1992. **5**(1): p. 27-34.
6. Pradhan, N. and P. Sadasivan, *The nature of dominant Lyapunov exponent and attractor dimension curves of EEG in sleep.* Computers in biology and medicine, 1996. **26**(5): p. 419-428.
7. Röschke, J. and J. Aldenhoff, *A nonlinear approach to brain function: deterministic chaos and sleep EEG.* Sleep, 1992. **15**(2): p. 95-101.
8. Pereda, E., et al., *Nonlinear behaviour of human EEG: fractal exponent versus correlation dimension in awake and sleep stages.* Neuroscience letters, 1998. **250**(2): p. 91-94.
9. Stêpieñ, R.A., *Testing for nonlinearity in EEG signal of healthy subjects.* Acta neurobiologiae experimentalis, 2002. **62**(4): p. 277-282.
10. Osborne, A.R. and A. Provenzale, *Finite correlation dimension for stochastic systems with power-law spectra.* Physica D: Nonlinear Phenomena, 1989. **35**(3): p. 357-381.
11. Stepien, R. and W. Klonowski. *Application of standard chaotic quantifiers for chemotherapy assessing by EEG-signal analysis*. in *Modelling and Simulation: a Tool for the Next Millennium, 13th European Simulation Multiconference ESM'99*. 1999. Warsaw.
12. Boon, M.Y., et al., *The correlation dimension: A useful objective measure of the transient visual evoked potential?* Journal of vision, 2008. **8**(1): p. 6-6.
13. Vialar, T., *Complex and chaotic nonlinear dynamics.* Advances in Economics and Finance, Mathematics and Statistics, Springer, 2009.

14. Grassberger, P. and I. Procaccia, *Measuring the strangeness of strange attractors*, in *The Theory of Chaotic Attractors*. 2004, Springer. p. 170-189.
15. Grebogi, C., E. Ott, and J.A. Yorke, *Chaos, strange attractors, and fractal basin boundaries in nonlinear dynamics.* Science, 1987. **238**(4827): p. 632-638.
16. Greenside, H., et al., *Impracticality of a box-counting algorithm for calculating the dimensionality of strange attractors.* Physical Review A, 1982. **25**(6): p. 3453.
17. Kugiumtzis, D., B. Lillekjendlie, and N.D. Christophersen, *Chaotic time series: Part 1: estimation of some invariant properties in state space.* Modeling, identification and control, 1994. **15**(4): p. 205-224.
18. Acharya, R., et al., *Nonlinear analysis of EEG signals at various sleep stages.* Computer methods and programs in biomedicine, 2005. **80**(1): p. 37-45.
19. Rodriguez-Bermudez, G. and P.J. Garcia-Laencina, *Analysis of EEG signals using nonlinear dynamics and chaos: a review.* Applied mathematics & information sciences, 2015. **9**(5): p. 2309.
20. Kemp, B., et al., *Analysis of a sleep-dependent neuronal feedback loop: the slow-wave microcontinuity of the EEG.* IEEE Transactions on Biomedical Engineering, 2000. **47**(9): p. 1185-1194.
21. https://physionet.org/content/sleep-edf/1.0.0/.
22. Kanwal, S., et al. *An image based prediction model for sleep stage identification*. in *2019 IEEE International Conference on Image Processing (ICIP)*. 2019. IEEE.
23. Ghasemzadeh, P., et al., *Classification of sleep stages based on LSTAR model.* Applied Soft Computing, 2019. **75**: p. 523-536.
24. Yildirim, O., U.B. Baloglu, and U.R. Acharya, *A deep learning model for automated sleep stages classification using PSG signals.* International journal of environmental research and public health, 2019. **16**(4): p. 599.
25. Liu, J., et al., *Automatic Sleep Staging Algorithm Based on Random Forest and Hidden Markov Model.* Computer Modeling in Engineering & Sciences, 2020. **123**(1): p. 401-426.
26. Janjarasjitt, S., *Nonlinear dynamical analysis: application to EEG sleep analysis.* วารสาร วิชาการ วิศวกรรมศาสตร์ ม. อบ., 2016. 4(1): p. 65-80.
27. Li, X., C. Ren, and X. Zou. *Sleep Staging Based on Energy and Complexity Characteristics of Sleep EEG Signals*. in *Journal of Physics: Conference Series*. 2019. IOP Publishing.
28. Peker, M., *An efficient sleep scoring system based on EEG signal using complex-valued machine learning algorithms.* Neurocomputing, 2016. **207**: p. 165-177.
29. Zhao, D., et al., *Comparative analysis of different characteristics of automatic sleep stages.* Computer methods and programs in biomedicine, 2019. **175**: p. 53-72.
30. Karrer, T.M., et al., *A practical guide to methodological considerations in the controllability of structural brain networks.* Journal of neural engineering, 2020. **17**(2): p. 026031.
31. Whitney, K., et al., *Systems theory as a foundation for governance of complex systems.* International Journal of System of Systems Engineering, 2015. **6**(1-2): p. 15-32.

32. Clark, J.B. and D.R. Jacques, *Practical measurement of complexity in dynamic systems.* Procedia Computer Science, 2012. **8**: p. 14-21.
33. Supratak, A., et al., *DeepSleepNet: A model for automatic sleep stage scoring based on raw single-channel EEG.* IEEE Transactions on Neural Systems and Rehabilitation Engineering, 2017. **25**(11): p. 1998-2008.
34. Tsinalis, O., et al., *Automatic sleep stage scoring with single-channel EEG using convolutional neural networks.* arXiv preprint arXiv:1610.01683, 2016.
35. Iber, C., *The AASM manual for the scoring of sleep and associated events: Rules.* Terminology and Technical Specification, 2007.
36. Feinberg, I. and T. Floyd, *Systematic trends across the night in human sleep cycles.* Psychophysiology, 1979. **16**(3): p. 283-291.
37. Achermann, P., et al., *A model of human sleep homeostasis based on EEG slow-wave activity: quantitative comparison of data and simulations.* Brain research bulletin, 1993. **31**(1-2): p. 97-113.
38. Kennel, M.B., R. Brown, and H.D. Abarbanel, *Determining embedding dimension for phase-space reconstruction using a geometrical construction.* Physical review A, 1992. **45**(6): p. 3403.
39. Fraser, A.M. and H.L. Swinney, *Independent coordinates for strange attractors from mutual information.* Physical review A, 1986. **33**(2): p. 1134.
40. Dijk, D.-J., et al., *Sleep extension in humans: sleep stages, EEG power spectra and body temperature.* Sleep, 1991. **14**(4): p. 294-306.
41. Fay, M.P. and M.A. Proschan, *Wilcoxon-Mann-Whitney or t-test? On assumptions for hypothesis tests and multiple interpretations of decision rules.* Statistics surveys, 2010. **4**: p. 1.
42. Zimmerman, D.W., *Invalidation of parametric and nonparametric statistical tests by concurrent violation of two assumptions.* The Journal of experimental education, 1998. **67**(1): p. 55-68.
43. Conover, W.J., *Practical nonparametric statistics*. Vol. 350. 1998: John Wiley & Sons.
44. Marsaglia, G., W.W. Tsang, and J. Wang, *Evaluating Kolmogorov's distribution.* Journal of statistical software, 2003. **8**(18): p. 1-4.
45. McGreevy, K.M., et al., *Using median regression to obtain adjusted estimates of central tendency for skewed laboratory and epidemiologic data.* Clinical chemistry, 2009. **55**(1): p. 165-169.
46. Seo, S., *A review and comparison of methods for detecting outliers in univariate data sets*. 2006, University of Pittsburgh.
47. Nobukawa, S., et al., *Classification methods based on complexity and synchronization of electroencephalography signals in Alzheimer's disease.* Frontiers in psychiatry, 2020. **11**.
48. Pace-Schott, E.F. and J.A. Hobson, *The neurobiology of sleep: genetics, cellular physiology and subcortical networks.* Nature reviews neuroscience, 2002. **3**(8): p. 591-605.
49. Winterhalder, M., et al., *Comparison of linear signal processing techniques to infer directed interactions in multivariate neural systems.* Signal processing, 2005. **85**(11): p. 2137-2160.

50. Borbély, A.A., et al., *The two-process model of sleep regulation: a reappraisal.* Journal of sleep research, 2016. **25**(2): p. 131-143.
51. Hassan, A.R. and M.I.H. Bhuiyan, *Automatic sleep scoring using statistical features in the EMD domain and ensemble methods.* Biocybernetics and Biomedical Engineering, 2016. **36**(1): p. 248-255.
52. Cerna, M. and A.F. Harvey, *The fundamentals of FFT-based signal analysis and measurement*. 2000, Application Note 041, National Instruments.
53. Liang, S.-F., et al., *Automatic stage scoring of single-channel sleep EEG by using multiscale entropy and autoregressive models.* IEEE Transactions on Instrumentation and Measurement, 2012. **61**(6): p. 1649-1657.
54. Corsi-Cabrera, M., et al., *power and coherent oscillations distinguish REM sleep, stage 1 and wakefulness.* International Journal of Psychophysiology, 2006. **60**(1): p. 59-66.
55. Zhu, G., Y. Li, and P. Wen, *Analysis and classification of sleep stages based on difference visibility graphs from a single-channel EEG signal.* IEEE journal of biomedical and health informatics, 2014. **18**(6): p. 1813-1821.
56. Altevogt, B.M. and H.R. Colten, *Sleep disorders and sleep deprivation: an unmet public health problem.* 2006.
57. Carskadon, M.A. and W.C. Dement, *Normal human sleep: an overview.* Principles and practice of sleep medicine, 2005. **4**: p. 13-23.

8. Author contributions statement

Seyed Mohammad Reza Hashemi Gholpayeghani: Project administration, Conceptualization, Methodology, Supervision, Validation

Mahmoud Alipour: Conceptualization, Methodology, Software, Data curation, Writing-Original draft preparation, Visualization, Investigation, Editing

9. Additional Information

The authors declare no competing interests.